Models of plasma and polarized particle transportation in SPI

A.A. Stepanenko[1], V.V. Fimushkin[2], A.N. Solovev[2], K.A. Ivshin[2], M.V. Kulikov[2], A.S. Belov[3], V.I. Davydenko[4], A.N. Zelensky[5]

[1]Plasma Physics Department
National Research Nuclear University MEPhI
115409 Moscow, Kashirskoe highway, 31, Russia
[2]Joint Institute for Nuclear Research, Dubna, Moscow region, Russia
[3]Institute for Nuclear Research of RAS, Moscow, Russia
[4]Institute of Nuclear Physics, Siberian Branch of the Russian Academy of Sciences, Novosibirsk Russia
[5]Moscow Institute of Physics and Technology, Phystech, Dolgoprudny, Moscow region, Russia

18.02.2026

Motivation I

- One of the routes to optimizing the Source of Polarized Ions (SPI) is by using the numerical modeling of plasma and polarized particle transport through the machine.
- A number of models describing dynamics of plasma in the SPI charge-exchange ionizer were developed for the purpose [JINR tech reports 2024, 2025]:
  - single-fluid ambipolar,
  - single-fluid electromagnetic,
  - multi-fluid ambipolar.
- In what follows, we summarize the main results and conclusions that were drawn from simulations within these models.

Single-fluid ambipolar model of plasma transport I

- The sketch of the SPI charge-exchange ionizer:

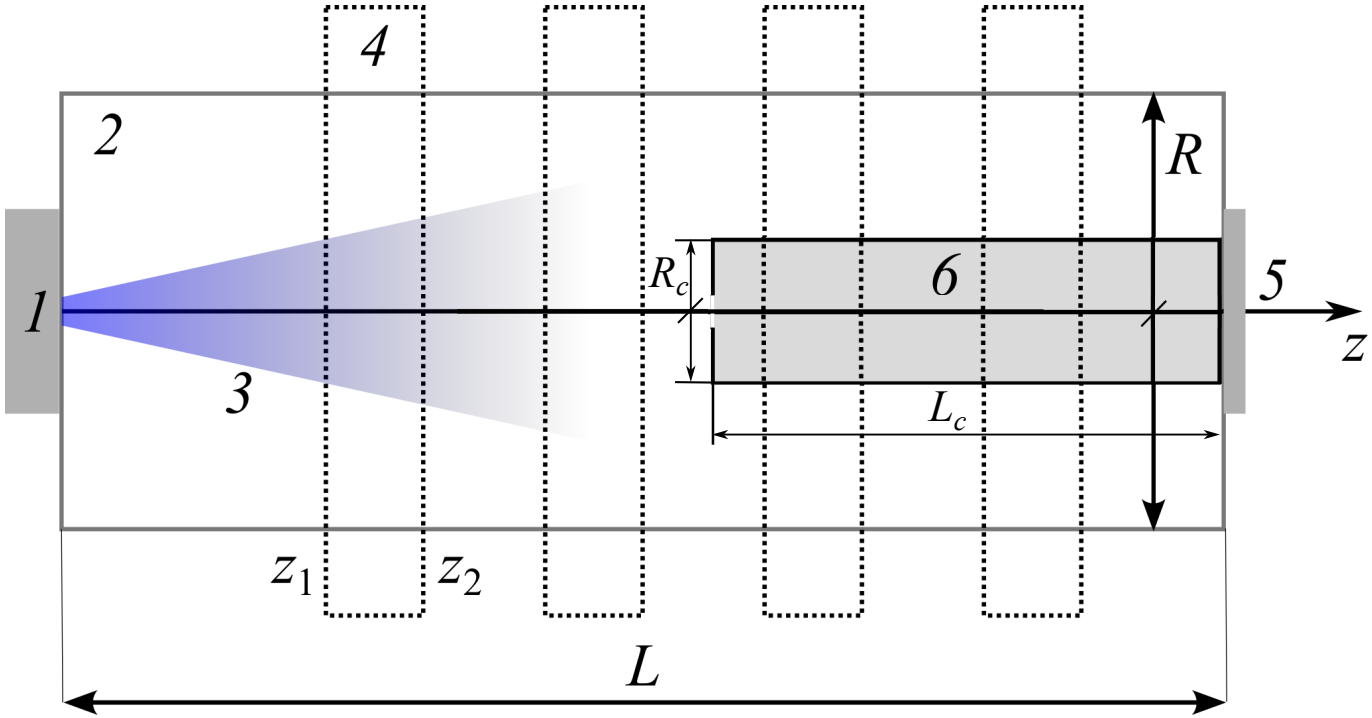

Figure: 1 – plasma source (ionizer), 2 – charge-exchange chamber, 3 – plasma flow, 4 – magnetic coils, 5 – extractor, 6 – storage cell.

Single-fluid ambipolar model of plasma transport II

- The basic assumptions put into the model:
  - plasma comprises electrons and ions of the single species,
  - electrons are "glued" to ions leading to zero net current, $\mathrm{J} = 0$,
  - energy transport: the polytropic index formalism, $\gamma_i = 5/3$, $\gamma_e \approx 1$,
  - plasma dynamics are described by the set of single-fluid MHD equations:

$$\frac{\partial n}{\partial t} + \nabla \cdot (n\mathrm{V}) = 0, \tag{1}$$

$$\frac{\partial T_i}{\partial t} + \mathrm{V} \cdot \nabla T_i + (\gamma_i - 1) T_i \nabla \cdot \mathrm{V} = 0, \tag{2}$$

$$\frac{\partial T_e}{\partial t} + \mathrm{V} \cdot \nabla T_e + (\gamma_e - 1) T_e \nabla \cdot \mathrm{V} = 0, \tag{3}$$

$$m_i n \left(\frac{\partial \mathrm{V}}{\partial t} + \mathrm{V} \cdot \nabla \mathrm{V} \right) = -\nabla (p_e + p_i) - 0.71 n \nabla T_e + \omega_{ci} \mathrm{V} \times \mathrm{b}. \tag{4}$$

  - no plasma recycling at the walls – hydrodynamic boundary conditions on all plasma parameters at the installation walls, $\partial_n f = 0$, $V_n = 0$, $\partial_n V_\tau = 0$.

Single-fluid ambipolar model of plasma transport III

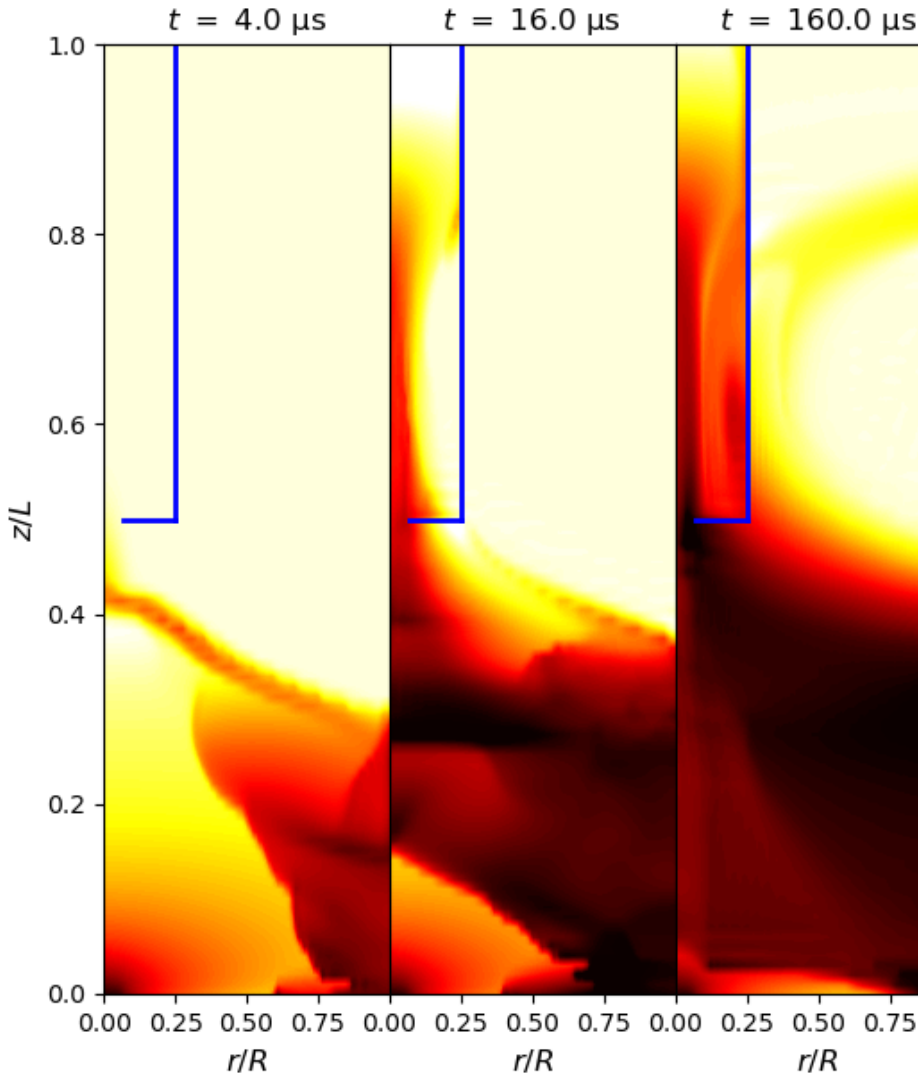

Figure: Dynamics of the plasma density in SPI.

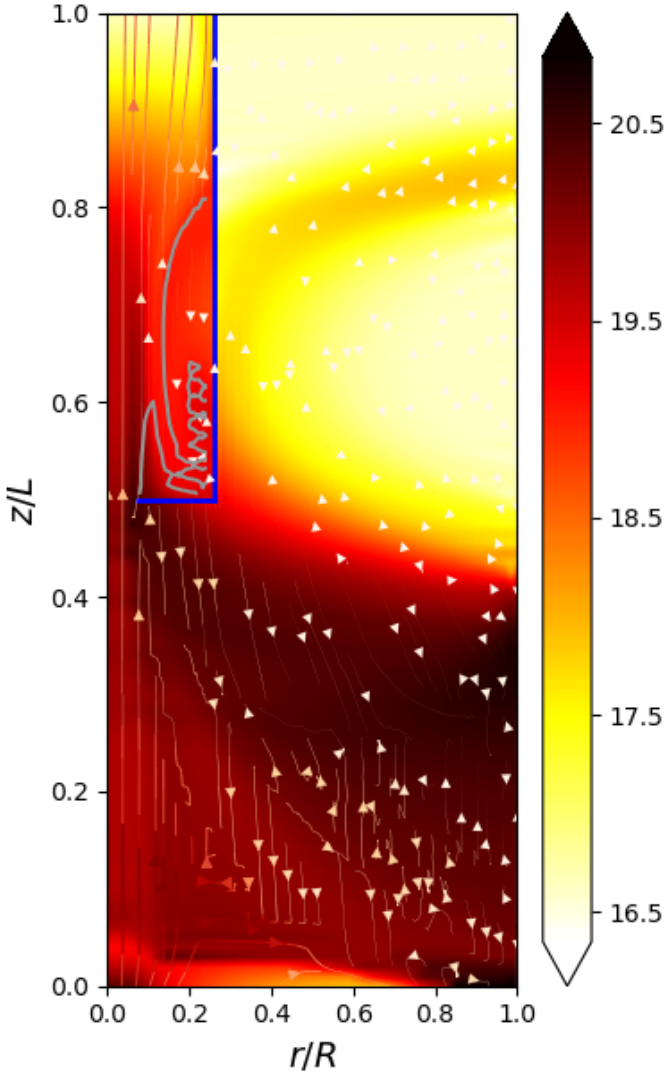

Figure: Plasma flow streamlines in the SPI chamber.

Single-fluid ambipolar model of plasma transport IV

- The main conclusions from simulations:
  - plasma is transported inside the storage cell within a thin axial channel,
  - upon traversing the magnetic mirror the plasma flow expands, potentially forming a gas target at the IOS aperture,
  - the flow conductivity of the magnetic mirror is limited $\longrightarrow$ not all plasma is transported into the storage cell – the reflected flow forms a macro-vortex.
- The model deficiencies:
  - no neutrals and polarized particles,
  - the inherent ambipolar assumption – however, electrons can potentially detach from ions $\longrightarrow J \neq 0$.

Single-fluid electromagnetic model of plasma transport I

- The electromagnetic model was created to test the validity of the ambipolar approximation and is built on the following assumptions:
  - plasma is two-component, electrons and ions of the single species,
  - no ambipolar approximation, the plasma current J is allowed to evolve,
  - energy transport is described with the polytropic index formalism,

Single-fluid electromagnetic model of plasma transport II

- ion dynamics are described by the set of MHD equations coupled to the Faraday's law:

$$\frac{\partial n}{\partial t} + \nabla \cdot (n\mathbf{V}) = 0, \tag{5}$$

$$m_i n \left(\frac{\partial \mathbf{V}}{\partial t} + \mathbf{V} \cdot \nabla \mathbf{V} \right) = -\nabla \left(p_i + p_e + \frac{B^2}{2\mu_0} \right) - 0.71 n \nabla T_e + \frac{1}{\mu_0} \mathbf{B} \cdot \nabla \mathbf{B} + \frac{1}{\mu_0} \nabla \times \mathbf{B} \times \mathbf{B}_0, \tag{6}$$

$$\frac{\partial T_e}{\partial t} + \mathbf{V} \cdot \nabla T_e + (\gamma_e - 1) T_e \nabla \cdot \mathbf{V} = 0, \tag{7}$$

$$\frac{\partial T_i}{\partial t} + \mathbf{V} \cdot \nabla T_i + (\gamma_i - 1) T_i \nabla \cdot \mathbf{V} = 0, \tag{8}$$

$$\frac{\partial \mathbf{B}}{\partial t} = \nabla \times \mathbf{V} \times (\mathbf{B} + \mathbf{B}_0) - \frac{1}{\mu_0} \nabla \times \rho \times \nabla \times \mathbf{B} + D_m \Delta \mathbf{B}. \tag{9}$$

- no plasma recycling at the walls $\longrightarrow$ hydrodynamic boundary conditions at the installation walls.

Single-fluid electromagnetic model of plasma transport III

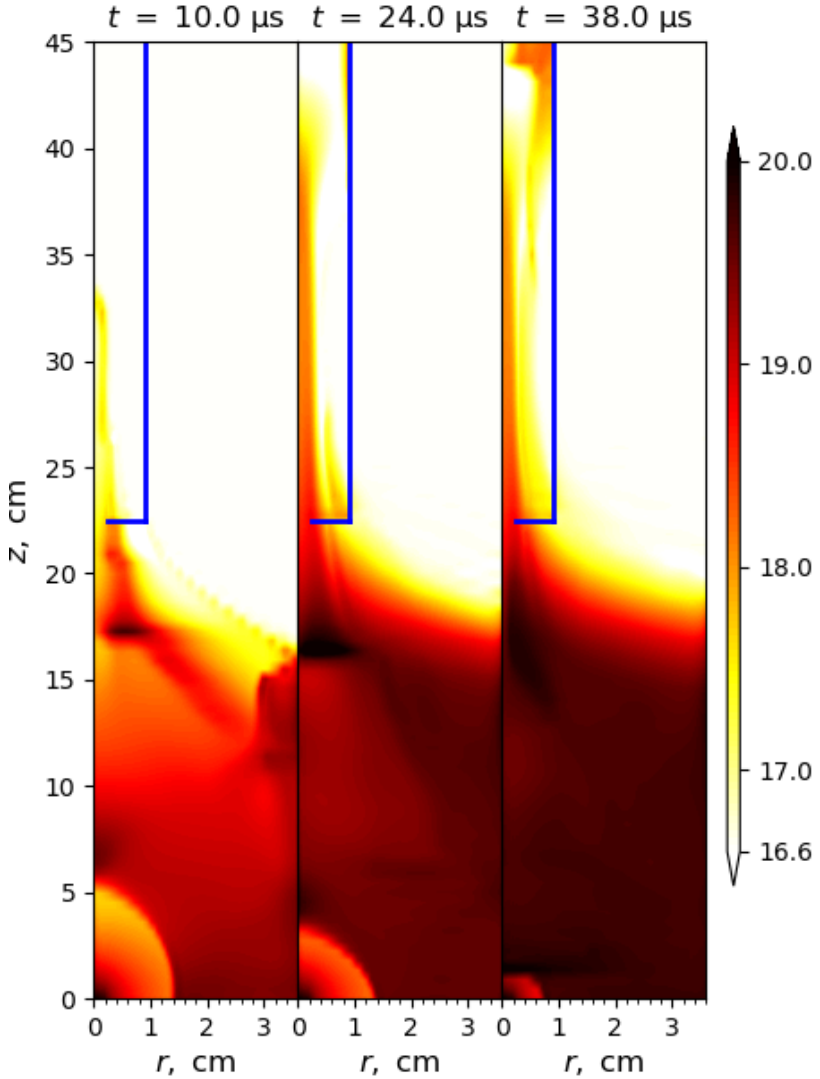

Figure: Dynamics of the plasma density in the AM approximation.

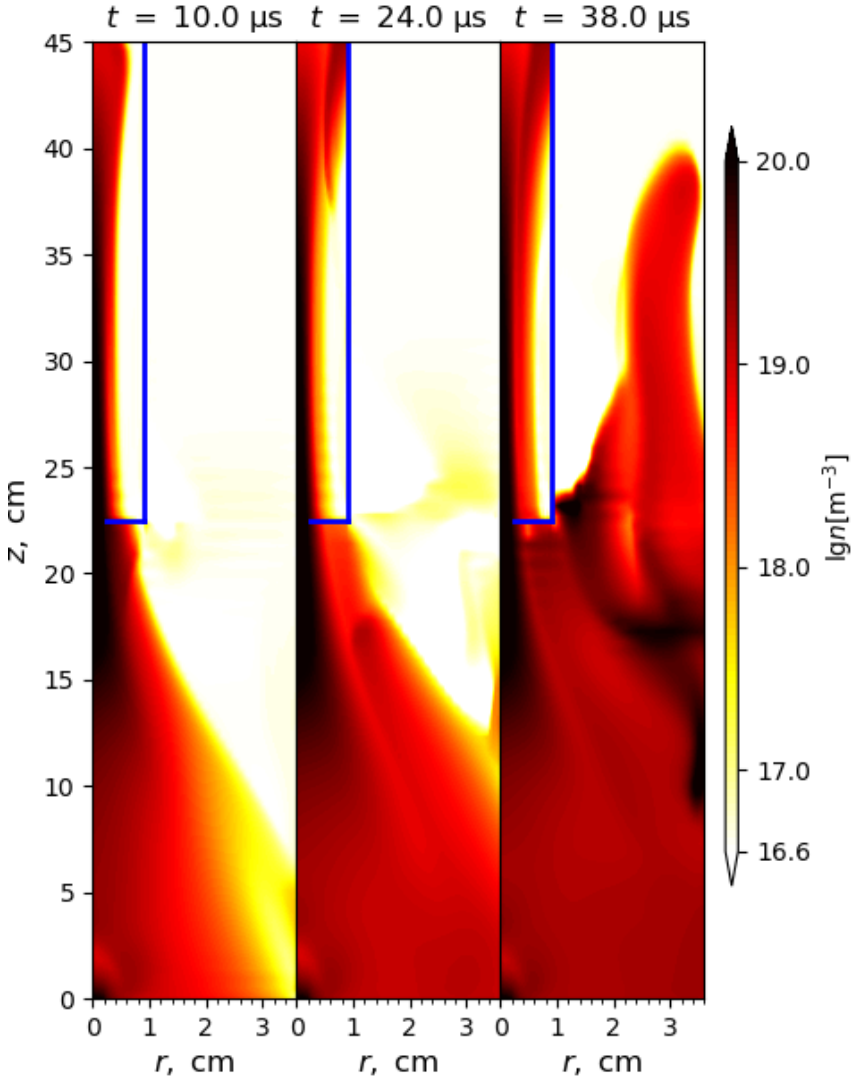

Figure: Dynamics of the plasma density in the EM approximation.

Single-fluid electromagnetic model of plasma transport IV

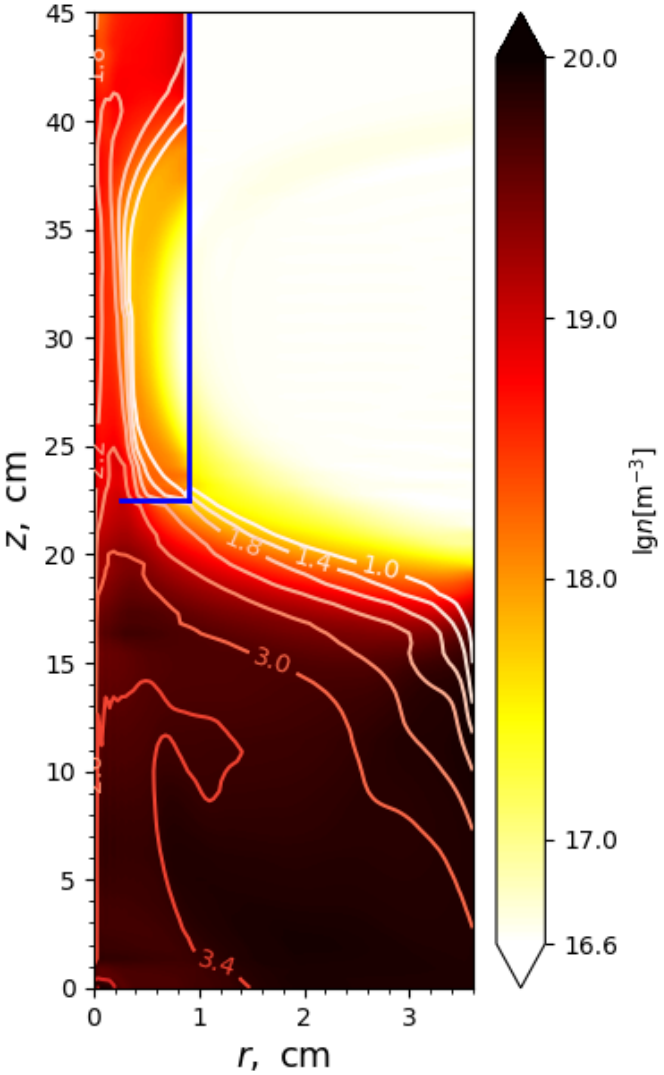

Figure: The electron temperature and density profiles in the AM limit.

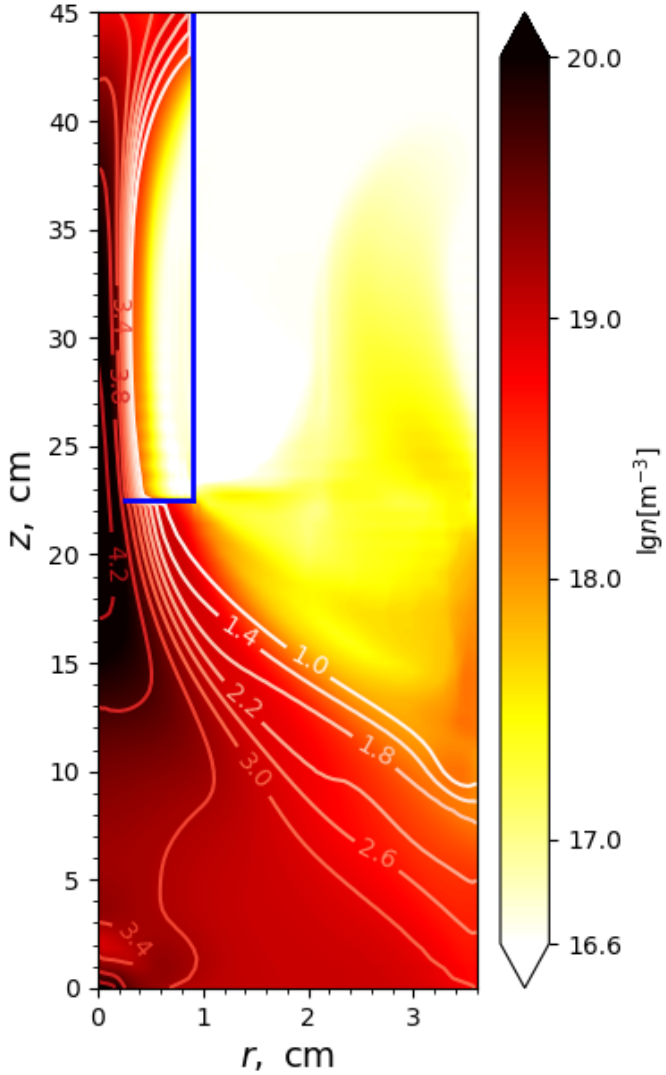

Figure: The electron temperature and density profiles in the EM limit.

Single-fluid electromagnetic model of plasma transport V

- The main conclusions from simulations:
  - the plasma flow is very similar to the ambipolar case, with plasma flow pattern being slightly different from the ambipolar limit (may be the result of the Hall effect absent from the model),
  - the plasma flow sieves through the magnetic field due to plasma diffusion,
  - EM and AM models produce close results $\longrightarrow$ hence we can use the less-costly AM model.
- The model deficiencies:
  - single-fluid – no neutrals and polarized particles,
  - no Hall effect (destabilizes simulation in curvilinear magnetic field configuration),
  - flow unstable at $t \sim 0.2 t_p$ due to boundary modes in a non-homogeneous magnetic field.

Multi-fluid ambipolar model of plasma transport I

- The model extends the single-fluid ambipolar model by including polarized particles and neutrals:
  - five-component plasma: electrons, main ions and neutrals, polarized ions and neutrals,
  - inelastic collisions: charge-exchange between main and polarized ion/neutrals, electron impact ionization and three-body recombination,
  - the ambipolar approximation $\longrightarrow$ electrons move with the ion velocity,
  - polarized and main ions have the same velocity (to stabilize the numerical scheme),
  - energy transport is described with the polytropic index formalism,
  - plasma recycling at the walls (the Bohm boundary conditions) is available,
  - no friction force between particles in the MHD limit to ensure numerical stability,
  - particle dynamics are governed by the following set of equations:

Multi-fluid ambipolar model of plasma transport II

$$\frac{\partial n_i}{\partial t} + \nabla \cdot (n_i \mathbf{V}_i) = -n_i n_{p\mathbf{0}} S_{CX,ip\mathbf{0}} + n_{i\mathbf{0}} n_p S_{CX,i\mathbf{0}p} + n_e n_{i\mathbf{0}} S_i - n_i n_e^2 S_r, \tag{10}$$

$$\frac{\partial \mathbf{V}_i}{\partial t} + \mathbf{V}_i \cdot \nabla \mathbf{V}_i = -\frac{1}{n_i m_i}\left(\nabla p_i + \frac{n_i}{n_i + n_p}\nabla p_e\right) - 0.71\frac{\nabla T_e}{m_i} + \omega_{ci}\mathbf{V}_i \times \mathbf{b} - \frac{m_p}{m_i + m_p}\nu_{ip}\left(\mathbf{V}_i - \mathbf{V}_p\right) - \frac{1}{2}\nu_{ii\mathbf{0}}\left(\mathbf{V}_i - \mathbf{V}_{i\mathbf{0}}\right). \tag{11}$$

$$\frac{\partial T_i}{\partial t} + \mathbf{V}_i \cdot \nabla T_i + \left(\gamma_i - 1\right) T_i \nabla \cdot \mathbf{V}_i = - 2\frac{m_i m_p}{\left(m_i + m_p\right)^2}\nu_{ip}(T_i - T_p) - \frac{1}{2}\nu_{ii\mathbf{0}}\left(T_i - T_{i\mathbf{0}}\right), \tag{12}$$

$$\frac{\partial n_{i\mathbf{0}}}{\partial t} + \nabla \cdot (n_{i\mathbf{0}} \mathbf{V}_{i\mathbf{0}}) = n_i n_{p\mathbf{0}} S_{CX,ip\mathbf{0}} - n_{i\mathbf{0}} n_p S_{CX,i\mathbf{0},p} - n_e n_{i\mathbf{0}} S_i + n_i n_e^2 S_r, \tag{13}$$

$$\frac{\partial \mathbf{V}_{i\mathbf{0}}}{\partial t} + \mathbf{V}_{i\mathbf{0}} \cdot \nabla \mathbf{V}_{i\mathbf{0}} = -\frac{1}{n_{i\mathbf{0}} m_i}\nabla p_{i\mathbf{0}} - \frac{m_p}{m_i + m_p}\nu_{i\mathbf{0}p}\left(\mathbf{V}_{i\mathbf{0}} - \mathbf{V}_p\right) - \frac{1}{2}\nu_{i\mathbf{0}i}\left(\mathbf{V}_{i\mathbf{0}} - \mathbf{V}_i\right), \tag{14}$$

$$\frac{\partial T_{i\mathbf{0}}}{\partial t} + \mathbf{V}_{i\mathbf{0}} \cdot \nabla T_{i\mathbf{0}} + \left(\gamma_{i\mathbf{0}} - 1\right) T_{i\mathbf{0}} \nabla \cdot \mathbf{V}_{i\mathbf{0}} = - 2\frac{m_i m_p}{\left(m_i + m_p\right)^2}\nu_{i\mathbf{0}p}(T_{i\mathbf{0}} - T_p) - \frac{1}{2}\nu_{i\mathbf{0}i}\left(T_{i\mathbf{0}} - T_i\right), \tag{15}$$

Multi-fluid ambipolar model of plasma transport III

$$\frac{\partial n_p}{\partial t} + \nabla \cdot (n_p \mathrm{V}_p) = n_i n_{p\mathbf{0}} S_{CX,ip\mathbf{0}} - n_{i\mathbf{0}} n_p S_{CX,i\mathbf{0}p} + n_e n_{p\mathbf{0}} S_i - n_p n_e^2 S_r, \tag{16}$$

$$\begin{aligned}\frac{\partial \mathrm{V}_p}{\partial t} + \mathrm{V}_p \cdot \nabla \mathrm{V}_p = &-\frac{1}{n_p m_p}\left(\nabla p_p + \frac{n_p}{n_i + n_p}\nabla p_e\right) - 0.71\frac{\nabla T_e}{m_p} \\ &+ \omega_{cp}\mathrm{V}_p \times \mathrm{b} - \frac{m_i}{m_i + m_p}\nu_{pi}\left(\mathrm{V}_p - \mathrm{V}_i\right) - \frac{m_i}{m_i + m_p}\nu_{pi\mathbf{0}}\left(\mathrm{V}_p - \mathrm{V}_{i\mathbf{0}}\right).\end{aligned} \tag{17}$$

$$\begin{aligned}\frac{\partial T_p}{\partial t} + \mathrm{V}_p \cdot \nabla T_p + \left(\gamma_p - 1\right) T_p \nabla \cdot \mathrm{V}_p = \\ - 2\frac{m_i m_p}{\left(m_i + m_p\right)^2}\nu_{pi}(T_p - T_i) - 2\frac{m_i m_p}{\left(m_i + m_p\right)^2}\nu_{pi\mathbf{0}}(T_p - T_{i\mathbf{0}}),\end{aligned} \tag{18}$$

$$\frac{\partial n_{p\mathbf{0}}}{\partial t} + \nabla \cdot (n_{p\mathbf{0}} \mathrm{V}_{p\mathbf{0}}) = -n_i n_{p\mathbf{0}} S_{CX,ip\mathbf{0}} + n_{i\mathbf{0}} n_p S_{CX,i\mathbf{0}p} - n_e n_{p\mathbf{0}} S_i + n_p n_e^2 S_r, \tag{19}$$

$$\frac{\partial \mathrm{V}_{p\mathbf{0}}}{\partial t} + \mathrm{V}_{p\mathbf{0}} \cdot \nabla \mathrm{V}_{p\mathbf{0}} = -\frac{1}{n_{p\mathbf{0}} m_p}\nabla p_{p\mathbf{0}}. \tag{20}$$

$$\frac{\partial T_{p\mathbf{0}}}{\partial t} + \mathrm{V}_{p\mathbf{0}} \cdot \nabla T_{p\mathbf{0}} + \left(\gamma_{p\mathbf{0}} - 1\right) T_{p\mathbf{0}} \nabla \cdot \mathrm{V}_{p\mathbf{0}} = 0. \tag{21}$$

Multi-fluid ambipolar model of plasma transport IV

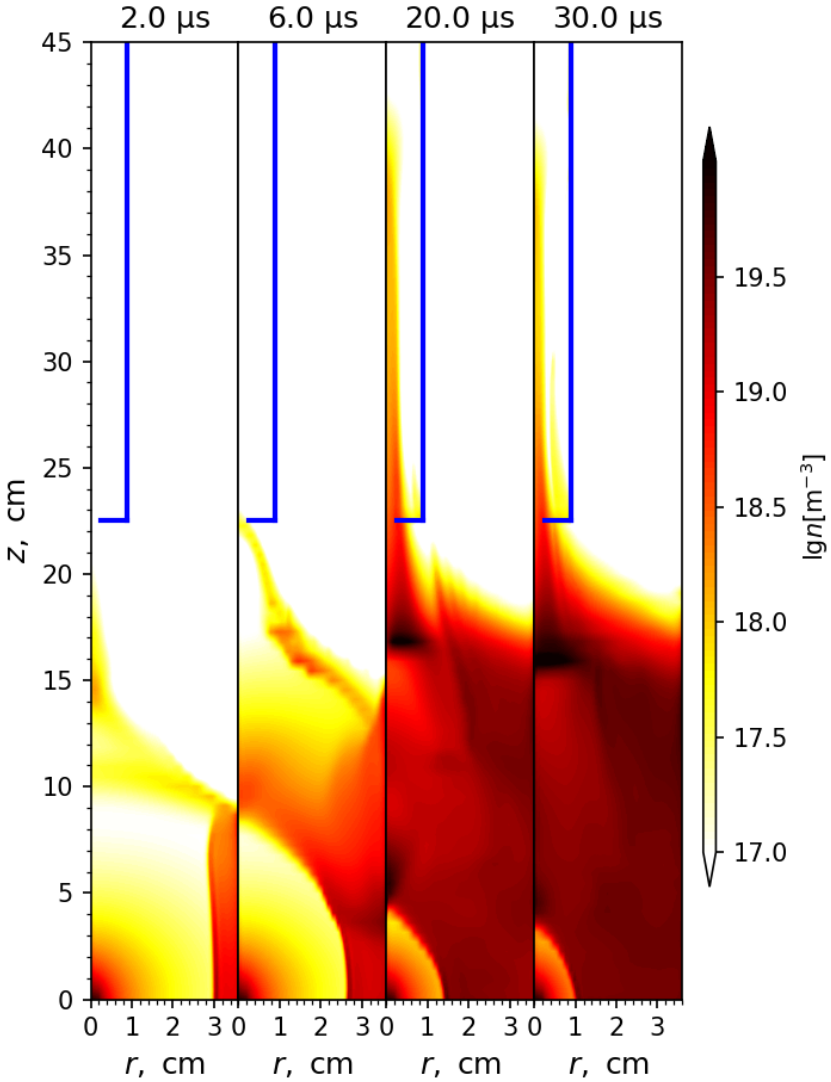

Figure: Dynamics of the plasma density in the HD approximation.

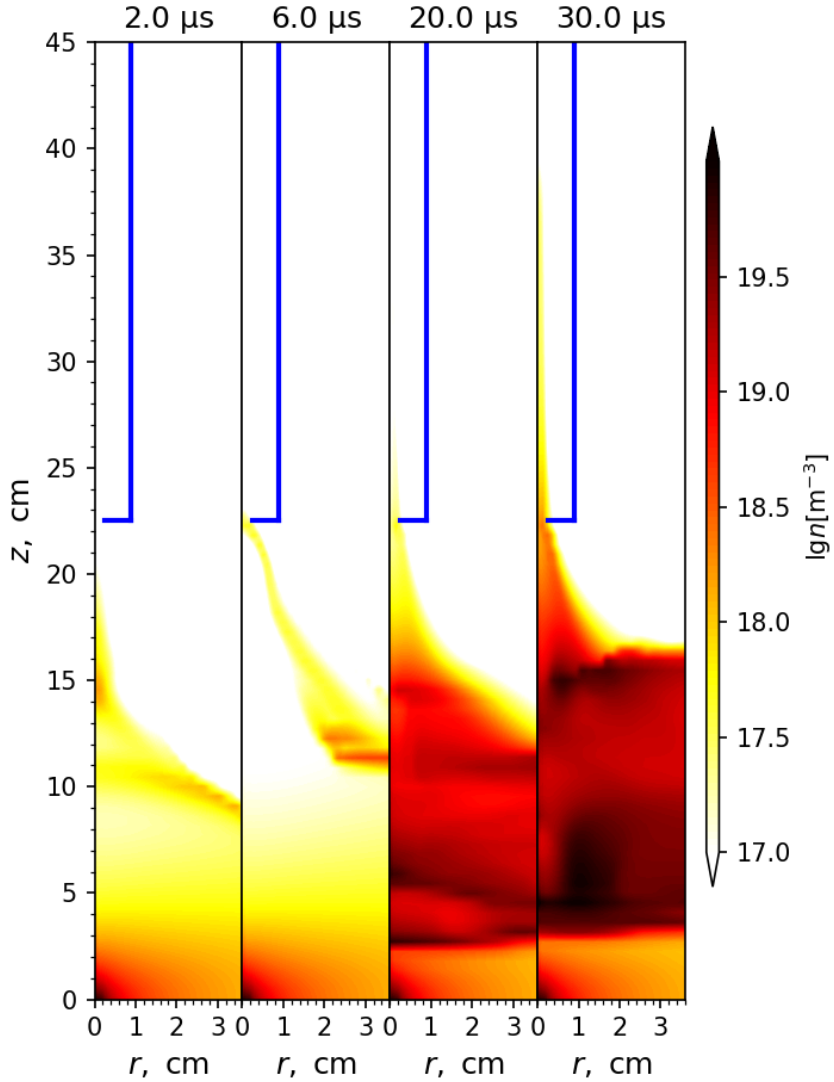

Figure: Dynamics of the plasma density in the MHD approximation.

Multi-fluid ambipolar model of plasma transport V

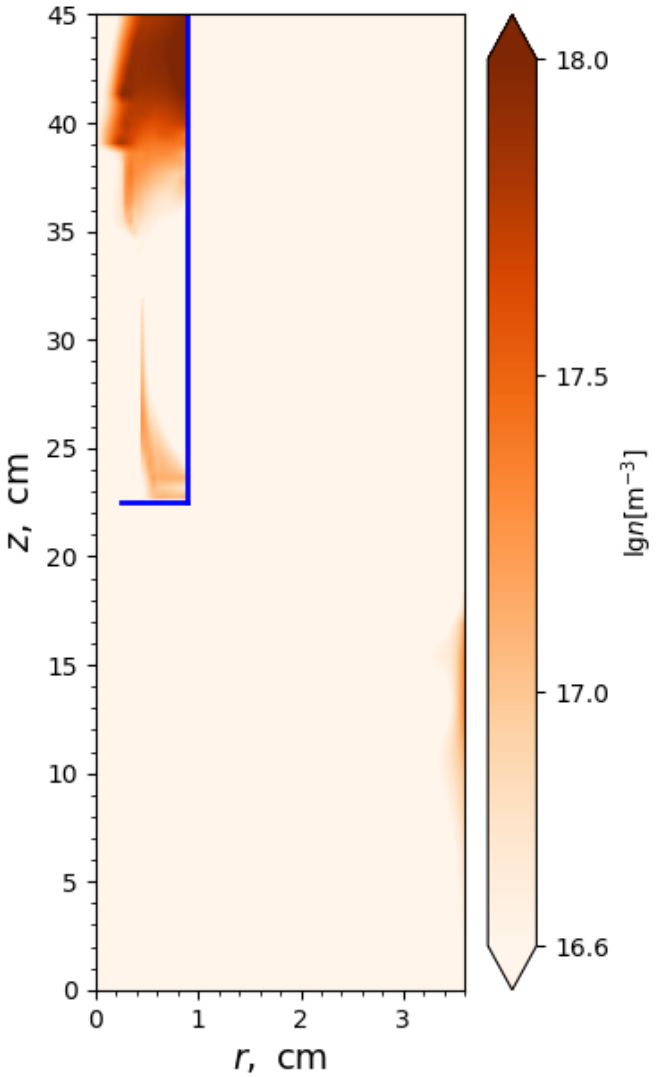

Figure: A snapshot of the polarized ion density in the HD limit.

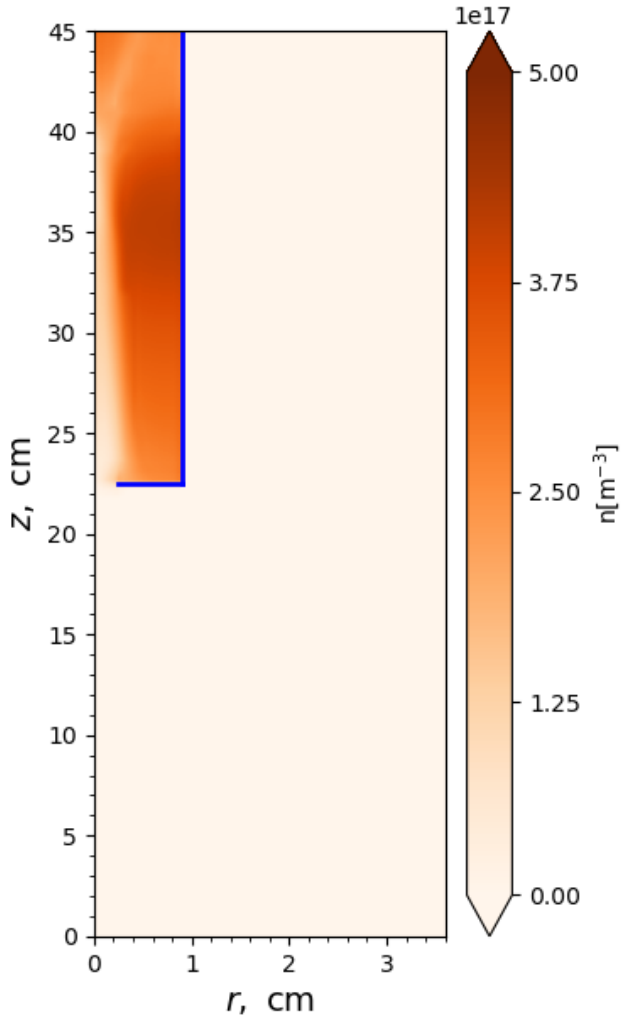

Figure: A snapshot of the polarized neutral density in the HD approximation.

Multi-fluid ambipolar model of plasma transport VI

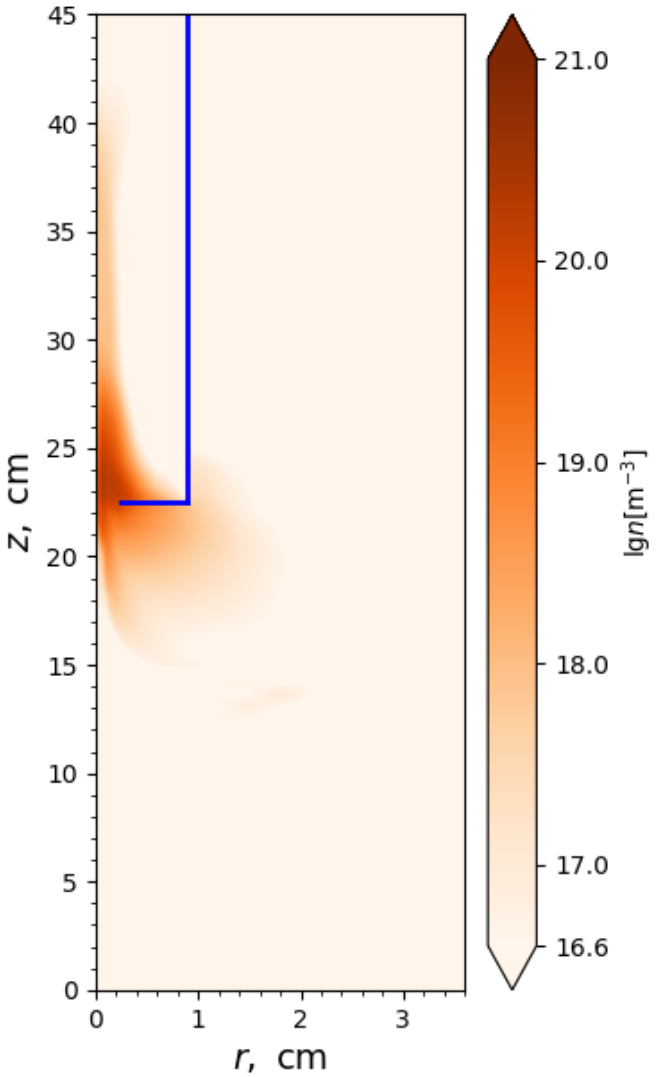

Figure: A snapshot of the polarized ion density in the MHD limit.

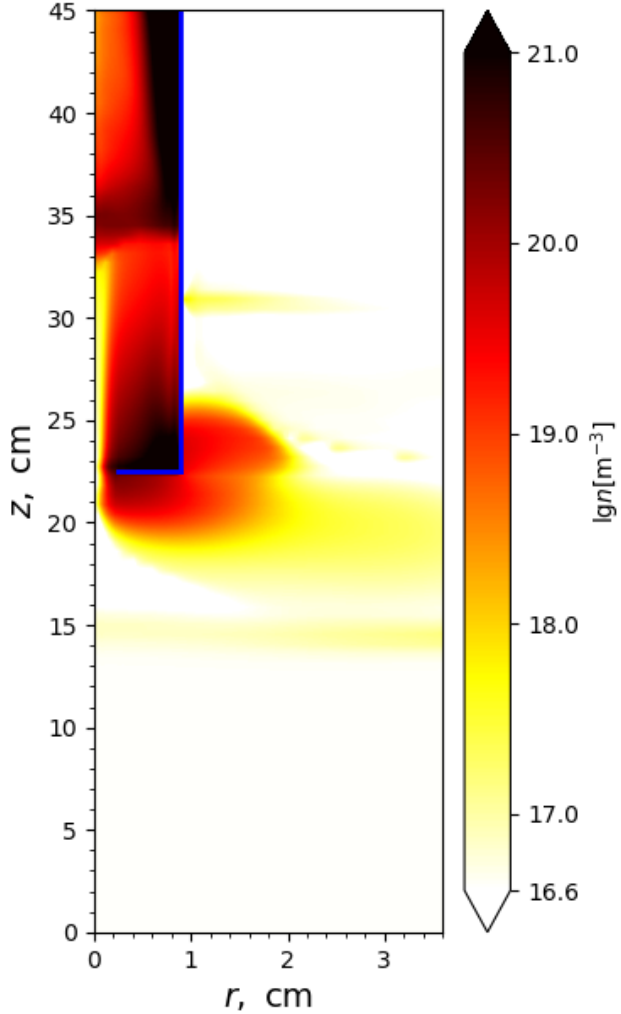

Figure: A snapshot of the main ion neutral density in the MHD approximation.

Multi-fluid ambipolar model of plasma transport VII

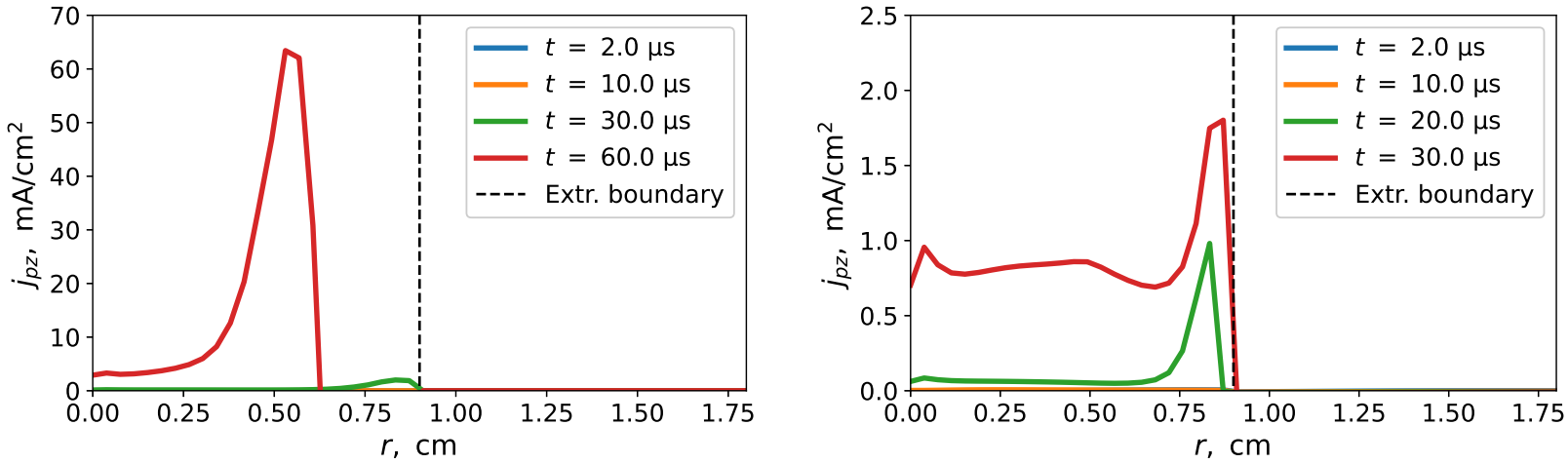

Figure: j_{pz} at the IOS in the HD (left) and MHD (right) limits.

- Total ion currents at $t = 30\ \mu s$ are $I_{pol}^{\mathrm{HD}} = 1.7$ mA, $I_{pol}^{\mathrm{MHD}} = 2.2$ mA.
- HD limit: j_{pz} is peaked at the storage cell wall and later on pushed from the surface.
- MHD limit: j_{pz} is peaked at the wall, but has a more homogeneous profile across the storage cell due to ion recycling at the wall. Taking the drag imposed by the main ion neutral layer into account would also push the flow from the wall.

Multi-fluid ambipolar model of plasma transport VIII

- The main conclusions from simulations:
  - the MHD limit:
    - ★ plasma flows in the storage cell through a thin channel, having 5-10% of the cell volume, limiting the neutral conversion and effectiveness,
    - ★ ion recycling at the inner wall of the storage cell produce a dense cloud of neutral particles sufficient to impose the drag force on the ion particles, leading to their accumulation within the cell,
  - the HD limit: turning the inelastic collisions on and imposing the friction forces does not drastically change the particle motion picture, compared to the basic AM limit $\longrightarrow$ the above AM-limit conclusions must persist.
- The model deficiencies:
  - the MHD version of the model is unstable at large t due to wall modes,
  - the HD version of the model does not correctly reproduce the ion recycling $\longrightarrow$ decreased accumulation of neutrals at the inner side of the storage cell wall.

Conclusions I

- A number of models were developed to describe plasma and polarized particle transportation through the SPI charge-exchange ionizer.
- Both ambipolar and non-ambipolar (electromagnetic) models demonstrated that the presence of the magnetic mirror in the SPI chamber forces the plasma flow through a thin channel with the effective diameter of $\sim 5-6$ mm, occupying $\approx 5-10\%$ of the storage cell volume. Small volume of the main plasma channel limits the effectiveness of the polarized particle conversion and extraction.
- Plasma expansion in the storage cell upon passing the magnetic mirror results in the formation of gas/plasma target at the IOS aperture as a result of the plasma-wall interaction. This area must hinder the extraction of the polarized particles.
- The magnetic mirror produces macro-vortices at the mirror entrance. These structures are unfavorable for the particle extraction.

Conclusions II

- The potential ways to increase the conversion of polarized neutrals into ions can be
  - through the optimization of the plasma feed into the storage cell by the aid of the moving diaphragms – a dynamic opening in the storage cell end to allow for a magnetically collimated plasma flow that is storage cell wide.
  - through re-organization of the plasma flow pattern, e.g. crossed transverse plasma and neutral beam injections [Belov, Zelenskii, JETP Letters 2025].

Thank you for attention!